References

1. Oxtoby, D. W. *Annu. Rev. Phys. Chem.* **1981**, *32*, 77.
2. Oxtoby, D. W. *Adv. Chem. Phys.* **1979**, *40*, 1.
3. Oxtoby, D. W. *Adv. Chem. Phys.* **1981**, *47*, 487.
4. Oxtoby, D. W. *J. Phy. Chem.* **1983**, *87*, 3028.
5. Rothschild, W. G. *Dynamics of Molecular Liquid*; John Wiley & Sons: **1984**.
6. Steele, D.; Yarwood. J. *Spectroscopy and Relaxation of Molecular Liquid*; Elsevier: **1991**.
7. Fischer, S. F.; Laubereau, A. *Chem. Phys. Lett.*, **1975**, *35*, 6.
8. Metiu, H.; Oxtoby, D.; Freed, K. F. *Phys. Rev.* **1977**, *15*, 361.
9. Schweizer, K.; Chandler, D. *J. Chem. Phys.* **1982**, *76*, 2296.
10. Jonas, J. *Acc. Chem. Res.* **1984**, *17*, 74.
11. Berens, P. H.; Wilson, K. R. *J. Chem. Phys.* **1981**, *74*, 4872.
12. Berens, P. H.; Mackay, D. H. J., White, G. M.; Wilson, K. R. *J. Chem. Phys.* **1983**, *79*, 2375.
13. Oxtoby, D. W.; Levesque, D.; Weis, J.-J. *J. Chem. Phys.* **1978**, *68*, 5528.
14. Levesque, D.; Weis, J.-J.; Oxtoby, D. W. *J. Chem. Phys.* **1980**, *72*, 2744.
15. Gussani, Y.; Levesque, D.; Weis, J.-J.; Oxtoby, D. W. *J. Chem. Phys.* **1982**, *77*, 2153.
16. Levesque, D., Weis, J.-J.; Oxtoby, D. W. *J. Chem. Phys.* **1983**, *79*, 917.
17. Chesnoy, J.; Weis, J. J. *J. Chem. Phys.* **1986**, *84*, 5378.
18. Allen, M. P.; Tildesley, D. J. *Computer Simulation of Liquids*; Clarendon, Oxford, **1987**.
19. Van Itterbeek, A.; Verbeke, O. *Physica* **1960**, *26*, 931.
20. Andersen, H. C.; Chandler, D.; Weeks, J. D. *Adv. Chem. Phys.* **1976**, *34*, 105.
21. Binder, K. *Monte Carlo Methods in Statistical Physics*; Springer-Verlag **1979**.

Study of Corrosion of Brass Coated Steel Cords in the Acetonitrile Solution of Sulfenamide Derivatives by Tafel Plot and AC Impedance Measurements

Young Chun Ko, Byung Ho Park[†], Hae Jin Kim[‡], Q Won Choi[#], Jongbaik Ree[*], and Keun Ho Chung[*]

Department of Chemistry, Chonnam National University, Kwangju 500-757

[†]*Kumho R & D Center, Kwangju 506-040*

[‡]*Department of Environmental Engineering, Dongshin University, Naju, Chonnam 520-714*

[#]*Department of Chemistry, Seoul National University, Seoul 151-742*

[*]*Department of Chemistry Education, Chonnam National University, Kwangju 500-757*

Received August 24, 1993

Corrosion of brass coated steel cords in the acetonitrile solution of sulfenamide derivatives, N-Cyclohexylbenzothiazole-2-sulfenamide (CBTS), N,N'-Dicyclohexylbenzothiazole-2-sulfenamide (DCBS), N-tert-Butylbenzothiazole-2-sulfenamide (TBBS), N-tert-Amylbenzothiazole-2-sulfenamide (TABS), and N-Oxydiethylbenzothiazole-2-sulfenamide (OBTS) was investigated by potentiostatic anodic and cathodic polarization (Tafel plot), DC polarization resistance, and AC impedance measurements. The corrosion current densities and rates are 1.236 $\mu A/cm^2$ and 0.655 MPY for CBTS; 1.881 $\mu A/cm^2$ and 0.988 MPY for DCBS; 2.367 $\mu A/cm^2$ and 1.257 MPY for TBBS; 3.398 $\mu A/cm^2$ and 1.809 MPY for TABS, respectively. OBTS among derivatives under study shows the lowest corrosion density (0.546 $\mu A/cm^2$) and the slowest corrosion rate (0.288 MPY). Also, the charge transfer resistances and the double layer capacitances are 275.21 $k\Omega \cdot cm^2$ and 7.0 $\mu F \cdot cm^{-2}$ for CBTS; 14.24 $k\Omega \cdot cm^2$ and 26 $\mu F \cdot cm^{-2}$ for DCBS; 54.15 $k\Omega \cdot cm^2$ and 16 $\mu F \cdot cm^{-2}$ for TBBS; 0.96 $k\Omega \cdot cm^2$ and 83 $\mu F \cdot cm^{-2}$ for TABS, respectively. The weaker the electron donating inductive effect of derivatives is and the smaller the effect of steric hindrance is, the more the corrosion of brass coated steel cords in the acetonitrile solution of sulfenamide derivatives is prevented. The above results agree with that observed in the field of tire industry.

Introduction

In recent years electrochemical techniques for rapid corrosion measurements are increasingly popular among corrosion workers, because long-term corrosion studies such as traditional weathering tests, weight-loss, and salt spray[1] can require hundreds of hours or even years to detect corrosion with any degree of precision and accuracy, but electrochemi-

Corrosion in the Acetonitrile Solution of Sulfenamide Derivatives

Bull. Korean Chem. Soc. **1994**, *Vol. 15, No. 2* 123

cal techniques require, at most, several hours. Electrochemical methods can also easily produce valuable mechanistic informations and data on both electrode capacitance and charge transfer kinetics for metals or alloys[2-4], steels[5-7], and batteries[8,9]. Thus, these are more suitable for examining corrosion mechanism and corroision rate.

On the other hand, a brass coated steel cord used as reinforcing material in rubber tire has been studied widely because of its increasing use.[10-13] During vulcanization in tire industry the sulfur combines chemically with brass thus insuring the necessary adhesion between cord and rubber. In this case, the sulfenamide derivatives have been mainly used as the vulcanizing material containing sulfur, because sulfenamide has many advantages as a vulcanizing material.[14] But, the vulcanizing material, sulfenamide also causes the corrosion of steel cords. Thus, it is important to elucidate which sulfenamide derivative is most suitable for the corrosion prevention.

The aim of the persent work is to examine the corrosion of brass coated steel cords in nonaqueous acetonitrile solutions of five sulfenamide derivatives, N-Cyclohexyl-benzothiazole-2-sulfenamide (CBTS), N,N'-Dicyclohexyl-benzothiazole-2-sulfenamide (DCBS), N-tert-Butylbenzothiazole-2-sulfenamide (TBBS), N-tert-Amylbenzothiazole-2-sulfenamide (TABS), and N-Oxydiethylbenzothiazole-2-sulfenamide (OBTS) by measuring corrosion current density, and corroision rate of these cords by Tafel plot and DC polarization resistance. Charge transfer resistance and double layer capacitance were also measured by AC impedance measurements.

Experimental

Materials. All sulfenamides were purchased from Wako Pure Chemical Industries, Ltd. and used without purification.

Solutions. Solutions are composed of sulfenamide derivatives and acetonitrile(CH_3CN). Acetonitrile was purchased from Wako Pure Chemical Industries, Ltd. and used without purification.

Steels. Brass coated steel cords (area=2 πrh : 0.716 cm^2, r=radius (0.19 mm), h=height) used are iron coated with the alloy of copper 64% and zinc 36%. The end section of steel cords (area=πr^2 : r=radius, 0.19 mm) was coverd by epoxy resin.

Tafel plot and DC polarization resistance. Tafel plot and DC polarization resistance measurements were made by immersing an electrode in an EG & G PARC Model cell under static conditions in nitrogen atmosphere. Tafel plot measurements were obtained individually by polarizing a working electrode either to +250 mV or to −250 mV with respect to corrosion potential (E_{corr}) at a scan rate 3 mV/s. A saturated silver-silver chloride electrode was used as a reference electrode via a salt bridge containing a saturated potassium chloride solution. The polorization resistance values were obtained by applying potentials to the working electrode ranging from −25 mV to +25 mV with respect to E_{corr} at a scan rate of 3 mV/s. The curves were compensated for the IR drop measuring the resistance between the reference electrode and specimen. The corrosion current densities were determined by using polarization resistance values and Tafel constants in an EG & G PARC Model cell under nitrogen atmosphere by using the following relation-

(a)

(b)
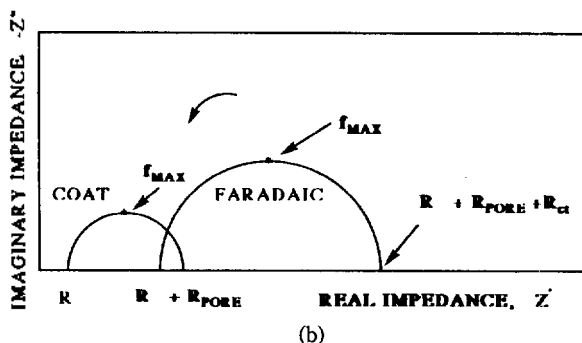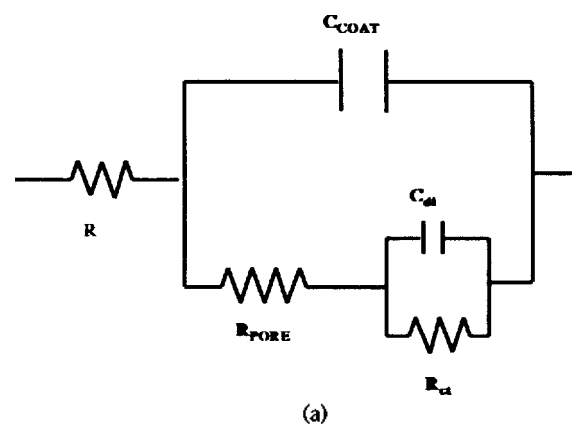
Figure 1. (a) Electrical equivalent circuit model for coated metal surface. C_{coat}=coating capacitance; C_{dl}=double-layer capacitance; R_Ω=solution resistance; R_{por}=coating pore resistance; R_{ct}=metal charge transfer resistance. (b) Cole-Cole plot of AC impedance. (Symbols are the same as Figure 1; $\omega=2\pi f$; f=frequency, Hz; Z=impedance)

ship[15]:

$$I_{corr}=\frac{(\beta_a)\,(\beta_c)}{2.3(R_p)\,(\beta_a+\beta_c)} \tag{1}$$

β_a =anodic Tafel constant (V/decade)
β_c =cathodic Tafel constant (V/decade)
R_p =polarization resistance (Ω/cm^2)
I_{corr} =corrosion current density (A/cm^2)

Once the I_{corr} was determined, the corrosion rate was calculated from the following equation[16]:

$$\text{Corrosion rate (MPY)}=\frac{0.13\ I_{corr}(E.W.)}{d} \tag{2}$$

$E.W.$ =equivalent weight at the corroding species (g)
d =density of the corroding species (g/cm^3)

AC impedence measurements. AC impedance was measured with EG & G PARC (Model 273) Potentiostat/Galvanostat and 5206 Lock-in-amplifier. The cell is consisted of saturated silver-silver chloride electrode, carbon electrode, and brass coated steel cord electrode as reference, auxiliary, and working electrode, respectively. Steel cords were produced by immersion for 20 minutes at a applied constant potential (DC −0.35 V). A common electrical equivalent circuit model for coated metal surface is shown in Figure 1(a). This corrosion R-C circuit is normally observed in lower frequency regions (0.01-100 Hz). The resistive element (R_{ct}) has been shown to be inversely proportional to he metallic corro-

124 *Bull. Korean Chem. Soc.* **1994**, *Vol. 15, No. 2*

Young Chun Ko et al.
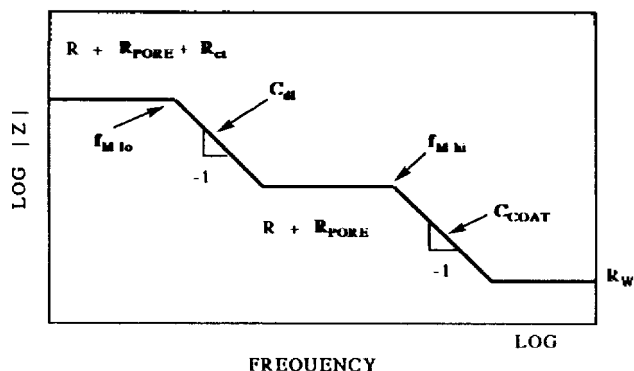
Figure 2. Bode plot of AC impedance. (Symbols are the same as Figure 1; $f_{M\ lo}$, $f_{M\ hi}$ breaking-point frequencies)

sion current and is considered to be the charge transfer resistance. This is helpful in supporting supplemental corrosion testing such as Tafel slope determinations. AC impedance for steel cords in the acetonitrile solution of OBTS was measured at a applied constant potential (DC -0.35 V) over the frequency range of 100 kHz to 0.01 Hz.

Impedance diagrams for the circuit presented in Figure 1(a) are shown in Figures 1(b) and 2, respectively.[17] Figure 1(b) represents the Cole-Cole plot where the impedance values at each frequency are resolved into the real and imaginary terms. In this figure, two semicircles intercept the real impedance axis at three points from which R_{ct}, R_{port} and R_Ω can be determined. Figure 2 represents the Bode plot, where we also determined R_{ct}, R_{port} and R_Ω by extrapolation and subtraction. Once a charge transfer resistance was determined, double layer capacitance C_{dl} can be calculated by the following Eq. (3):

$$\omega_{max} = \frac{1}{C_{dl}R_{ct}}, \quad \omega = 2\pi f, \tag{3}$$

where

R_{ct} = charge transfer resistance ($\Omega \cdot cm^2$)
C_{dl} = double layer capacitance ($F \cdot cm^{-2}$)
f = frequency in a maximum angular momentum
ω_{max} = maximum frequency at the maximum of the semicircle in the Cole-Cole plot

Results and Discussion

Results obtained by Tafel plot and DC polarization resistance are represented in Table 2. Figures 3 and 4 are Tafel plots of steel cord in a pure acetonitrile solution and the acetonitrile solution of OBTS, respectively. The corrosion current density (I_{corr}) is obtained by the intersection of the Tafel extrapolations of the anodic and cathodic branches of the polarization curves in Figures 3 and 4. The corrosion current density (I_{corr}) and rate are calculated using Eqs. (1) and (2), respectively. As shown in Table 2, the corrosion current density and rate for CBTS (1.236 μA/cm²; 0.655 MPY) are lower and slower than those for DCBS (1.881 μA/cm²; 0.988 MPY), respectively, and those for TBBS (2.367 μA/cm²; 1.257 MPY) lower and slower than those for TABS (3.398 μA/cm²; 1.809 MPY). If we abbreviate sulfenamide derivative as R₁-S-N-R ₂, CBTS has a cyclohexyl group in R₂ while DCBS has two

Table 1. Sulfenamide Derivatives

a.

N-Oxydiethylbenzothiazole-2-sulfenamide (OBTS)

b.

N-Cyclohexylbenzothiazole-2-sulfenamide (CBTS)

c.

N,N'-Dicyclohexylbenzothiazole-2-sulfenamide (DCBS)

d.

N-tert-Butylbenzothiazole-2-sulfenamide (TBBS)

e.

N-tert-Amylbenzothiazole-2-sulfenamide (TABS)

Table 2. Corrosion Data for Steel Cord in 1.00×10^{-3} M Acetonitrile Solution of Sulfenamide Derivatives from Tafel Plot and DC Polarization Resistance Measurements

Sulfenamide derivatives	E_o^* (mV)	β_a V/decade	β_c V/decade	I_{corr} (μA/cm²)	Corrosion rate (MPY)
Blank (CH₃CN)	-392	0.261	0.941	0.716	0.374
OBTS	-326	0.157	0.188	0.546	0.288
CBTS	-382	0.390	0.441	1.236	0.655
DCBS	-365	0.207	0.243	1.881	0.988
TBBS	-395	0.310	0.706	2.367	1.257
TABS	-352	0.459	0.659	3.398	1.809

*E_o represents the free corrosion potential *vs.* a saturated Ag-AgCl reference electrode.

cyclohexyl groups. Because cyclohexyl group is electron donating group, CBTS shows less electron donating inductive effect than DCBS. By the same reason, TBBS shows less electron donating inductive effect than TABS, because TBBS has a tert-butyl group in R₂ while TABS has a tert-amyl group. Therefore, we can consider that the weaker the electron donating inductive effect is, the lower corrosion current density is and the slower corroision rate is. Among the sulfenamide derivatives, OBTS has an oxydiethyl group, a electron withdrawing group or the weakest electron donating group, in R₂. So, it withdraws electrons from neighboring
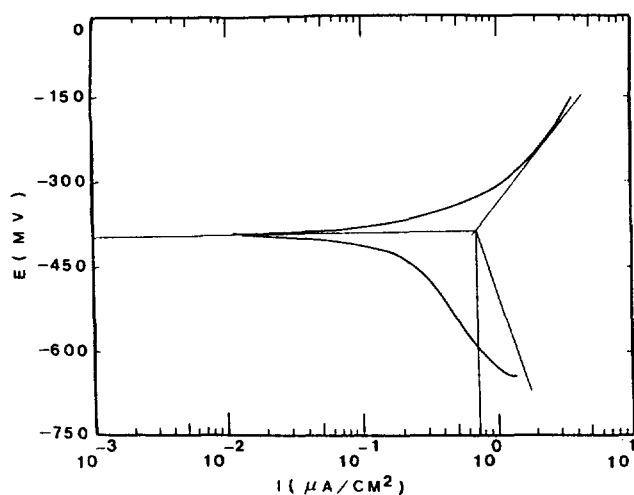
Corrosion in the Acetonitrile Solution of Sulfenamide Derivatives

Bull. Korean Chem. Soc. 1994, *Vol. 15, No. 2* 125

Figure 3. Tafel plot of steel cord in pure acetonitrile solution.
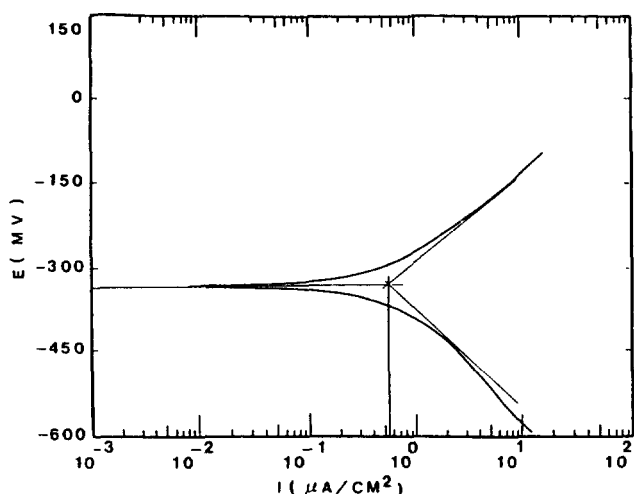
Figure 4. Tafel plot of steel cord in acetonitrile solution of 1.00 mM OBTS.

Figure 5. Cole-Cole plot of steel cord in acetonitrile solution of 1.00 mM CBTS.
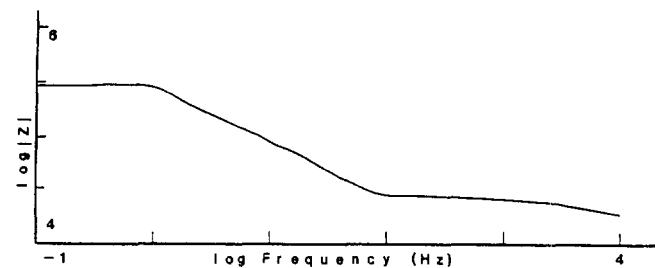
Figure 6. Bode plot of steel cord in acetonitrile solution of 1.00 mM CBTS.

Table 3. Corrosion Data for Steel Cord in 1.00×10^{-3} M Acetonitrile Solution of Sulfenamide Derivatives from AC Impedance Measurement

OBTS Concentration $(10^{-3}$ M)	R_{ct} $(k\Omega \cdot cm^2)$	C_{dl} $(\mu F \cdot cm^{-2})$
Blank (CH₃CN)	177.89	<1
OBTS	15.02	24
CBTS	275.21	7
DCBS	14.24	26
TBBS	54.15	16
TABS	0.96	83

N-atom or hardly donates electron to N-atom. As mentioned above, because the smaller the electron donating inductive effect is, the better prevention of corrosion is, OBTS shows the lowest corrosion current density and the slowest corrosion rate as shown in Table 2. Traditionally OBTS has been most widely used to vulcanize, which agrees with the present results. As a conclusion, the fewer electron donating groups in R_2 are, the more the corrosion is prevented.

On the other hand, it is interesting to consider the differences of corrosion densities and corrosion rates for sulfenamide derivatives in terms of steric hindrance. CBTS has a cyclohexyl group as R_2 in R_1-S-N-R_2 whereas DCBS has two cyclohexyl groups as mentioned above. Thus, DCBS has more steric hindrance than CBTS. In the similar way, TABS has more than that of TBBS. As shown in Table 2, the smaller the steric hindrance is, the lower a corrosion current density is and the slower a corrosion rate is. This is because the steric hindrance interfere the lone pair electrons in N-atom to bond with the proton. That is, the smaller the steric hindrance is, the better the lone pair electrons in N-atom bond with the proton, thus, the corrosion is more prevented.
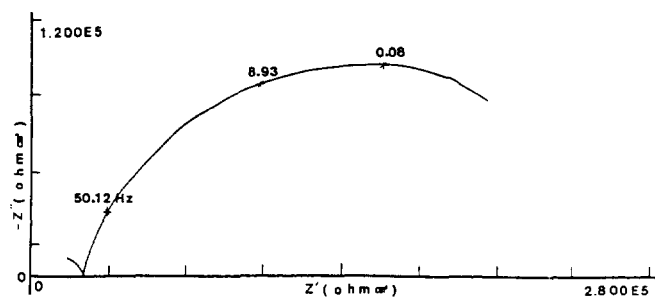
OBTS has a electronegative O-atom in R_2. Among the five sulfenamide derivatives, OBTS exhibits the most anticorrosion effect, which is caused by O-atom rather than by N-atom. That is because electronegative O-atom can bond with the proton better than N-atom.

In order to investigate the corrosion effect of sulfenamide derivatives in detail, we also measured AC impedances of the acetonitrile solution of sulfenamide derivatives. The AC impedance was measured at DC -350 mV, because the free corrosion potential for sulfenamide derivatives appears from -326 mV to -395 mV. Results obtained by AC impedance measurements are plotted in Figures 5 and 6 in the form of Cole-Cole and Bode plot, respectively. In Figure 6, the loci of the Cole-Cole plot (Figure 5) in the high- and low-frequency region is attributed to coat and faradaic R-C circuit, respectively.[17] The electrical equivalent circuit model used in this work is shown in Figure 1(a) as previously reported.[17] In Table 3, we listed charge transfer resistance (R_{ct}) and double-layer capacitance (C_{dl}) for the steel cord in the

126 *Bull. Korean Chem. Soc.* **1994**, *Vol. 15, No. 2*

Il-Wun Shim et al.

acetonitrile solution of sulfenamide derivatives, which were determined by analysis of Cole-Cole plot (Figure 5) and Bode plot (Figure 6). As mentioned in figure captions, Figures 5 and 6 are the CBTS cases. As shown in Table 3, the charge transfer resistance of CBTS (275.21 k$\Omega \cdot$cm^2) is larger than DCBS (14.24 k$\Omega \cdot$cm^2), TBBS (54.15 k$\Omega \cdot$cm^2) than TABS (0.96 k$\Omega \cdot$cm^2). Here, R_d is the characteristic of the corrosion resistance of electrode material in given solution.[18] That is, the larger R_d is, the better a corrosion resistance is. On the other hand, the double layer capacitance of CBTS (7.0 μF$\cdot$cm^{-2}) is smaller than DCBS (26 μF$\cdot$cm^{-2}), TBBS (16 μF$\cdot$cm^{-2}) than TABS (83 μF$\cdot$cm^{-2}). C_{dl} is the characteristic of the corrosion area. That is, the decrease of a double layer capacitance is due to the decrease in the corrosive area.[18] As a result, the weaker the electron donating inductive effect of derivatives is and the smaller the effect of steric hindrance is, the larger R_d is and the smaller C_{dl} is, thus, the more a corrosion is prevented. If we compare the results of corrosion current density and corrosion rate in Table 2 with the results of charge transfer resistance and double layer capacitance in Table 3, there are some differences in the corrosion effect of sulfenamide derivatives containing different functional group. That is because a charge transfer resistance at a applied constant potential is said to represent only cathodic current and not the corrosion rate itself.[15,19] That is, when we consider the corrosion effect of sulfenamide derivatives by comparing charge transfer resistances, we can explain the corrosion effect just for the case in which sulfenamide derivatives have the similar functional groups.

References

1. Altmayer, F. *Met. Fin.* **1987**, *83*, 57.

2. Schueller, G. R. T.; Taylor, S. R. *J. Electrochem. Soc.* **1992**, *139*, 3120.
3. Dobbelaar, J. A. L.; de Wit, J. H. W. *J. Electrochem. Soc.* **1990**, *137*, 2038.
4. Milosev, I.; Metikos-Hukovic, M. *Corrosion* **1992**, *48*, 185.
5. Sekine, I.; Sangbongi, M.; Hagiuda, H.; Oshibe, T.; Yuasa, M.; Imahama, T.; Shibata, Y.; Wake, T. *J. Electrochem. Soc.* **1992**, *139*, 3167.
6. Bonnel, A.; Dabosi, F.; Deslouis, C.; Duprat, M.; Keddam, M.; Tribollet, B. *J. Electrochem. Soc.* **1983**, *130*, 753.
7. Hedayat, A.; Postlethwaite, J.; Yannacopoulos, S. *Corrosion* **1992**, *48*, 1027.
8. Kelly, R. G.; Moran, P. J. *J. Electrochem. Soc.* **1987**, *134*, 31.
9. Downey, S. B.; Devereux, O. F. *J. Electrochem. Soc.* **1992**, *139*, 3129.
10. Van Ooij, W. J. V. *Surf. Sci.* **1977**, *68*, 1.
11. Ishikawa, Y.; Kawakami, S. *Rubber Chem. Technol.* **1985**, *59*, 1.
12. Natarajan, R.; Angelo, P.; Gerge, N.; Tamhankar, R. *Corrosion* **1975**, *31*, 302.
13. Walker, G. D. *Corrosion* **1977**, *33*, 262.
14. Zaucker, E.; Bogemann, M. U.S. Patent **1934**, 19286.
15. Rajagopal, V.; Iwasaki, I. *Corrosion* **1992**, *48*, 124.
16. EG & G PARC Application Note 148.
17. Murray, J. N.; Hack, H. P. *Corrosion* **1992**, *48*, 671.
18. Sekine, I.; Kohara, K.; Sugiyama, T.; Yuasa, M. *J. Electrochem. Soc.* **1992**, *139*, 3090.
19. Thompson, N. G.; Lawson, K. M.; Beavers, J. A. *NACE* **1988**, *44*, 585.

The Chemistry of Rhodium in Polysulfone: Reactions with Various Small Gas Molecules

Il-Wun Shim*, Jin-Si Kim, Seok-Jong Oh[†], Yong-Sik Yang[†], Hwan-Kyu Suh[†], and Sang-Kyu Lee[†]

Department of Chemistry, Chung-Ang University, Seoul 156-756
[†]*Agency for Defence Development of Korea, Taejon 306-600*

RhCl[P(C$_6$H$_5$)$_3$]$_3$ complexes have been incorporated in polysulfone (PS) as a dispersion medium using cosolvent (THF). The interactions between Rh(I) complexes and polysulfone polymer molecules are examined by infrared spectroscopy and thermal analysis. The chemical reactivity of Rh in PS films has been investigated by reacting Rh sites with CO, H$_2$, D$_2$, O$_2$, NO, C$_2$H$_2$ and C$_2$H$_4$ in the temperature range 25-200°C. Various Rh-carbonyl, -hydride and -nitrosyl species formed in PS films are characterized by their infrared spectra. Rh complexes in PS film show interesting catalytic reactivities in the reactions such as hydrogenation of C$_2$H$_2$ and C$_2$H$_4$, oxidation of CO, and reduction of NO by CO or H$_2$ gas under relatively mild conditions.

Introduction

Metal-containing polymeric materials have been a topic of considerable interest in recent years because of the burgeoning interests in search for new high-performance materials.[1-6] In addition, these materials have received much at-